Hydrogen Atom Addition to Cytosine, 1-Methylcytosine, and Cytosine−Water Complexes. A Computational Study of a Mechanistic Dichotomy

František Tureček* and Chunxiang Yao

Department of Chemistry, Bagley Hall, Box 351700, University of Washington, Seattle, Washington 98195-1700

Received: May 30, 2003; In Final Form: August 19, 2003

Combined ab initio and density functional theory calculations at the B3-MP2/6-311++G(3df,2p) level of theory are used to investigate the structures and energetics of radicals produced by hydrogen atom addition to cytosine tautomers, 1-methylcytosine, and cytosine−water complexes. H-atom adducts to the N-3 positions are the most stable radical isomers derived from cytosine tautomer (**1**), 1-methylcytosine, and cytosine−water complexes in the gas phase. Solvent effects on radical stabilities are addressed by calculations that use the polarizable continuum model. Solvation by bulk water favors C-5 and C-6 adducts which have free energies in water that are comparable to those of the N-3 adducts. H-atom additions to the C-5 positions have the lowest activation energies for all cytosine derivatives under study and are predicted to be kinetically predominant. H-atom additions to the N-3 and C-6 positions are solvent dependent. In the absence of solvation, N-3 is more reactive than C-6 in cytosine and 1-methylcytosine. Water complexation increases the activation energy for H-atom addition to N-3 and results in a reactivity reversal for the N-3 and C-6 positions.

Introduction

Radical additions to nucleobases represent an important component of the complex process of DNA radiation damage.[1,2] Among the several reactive species that are produced by radiolysis of water, hydrogen atoms can attack nucleobases forming H-atom adducts as transient radical intermediates. Alternatively, electron capture by the nucleobase forms an anion radical that upon protonation produces an H-atom adduct. The relative importance of these processes in DNA damage has been the subject of a discussion.[2] Radiolysis of cytosine, 1-methylcytosine, and cytidine-containing nucleotides has been shown by electron paramagnetic resonance (EPR) studies to produce transient radicals corresponding formally to H-atom addition to the C-5 and C-6 positions on the pyrimidine ring[3,4] of which the C-5 adduct predominated. Recently, the EPR data have been interpreted as also supporting the formation of an N-3 adduct from cytosine,[5,6] whereas adducts of O-2, C-4, and the 4-amino group have not been detected. However, irradiation of cytosine and derivatives in frozen lithium chloride glasses produced transient radical intermediates that were assigned by EPR to be either N-3 or NH_3 adducts.[7] Studies of OH radical addition to cytosine and derivatives shown dominant formation of C-5 adducts and minor C-6 adducts.[8]

The dichotomy in the experimental data for cytosine radicals raises the question of whether the C-5 and C-6 positions in cytosine are the intrinsically most reactive ones and the addition is kinetically controlled or whether the primary adducts undergo fast secondary reactions, so that the observed radicals are the least reactive and hence most stable intermediates. A related question concerns the effect of the medium, e.g., the solvent, dissolved ions, or other solutes, that can react with the primary radiolytic intermediates.

The *intrinsic* molecular properties of transient intermediates, including nucleobase[9] and heterocyclic radicals,[10] have been studied in the gas phase where solvent and other environmental effects are absent.[11,12] For example, recent experimental and computational studies of uracil radicals indicated that, among the hydrogen atom adducts, the C-5 radical derived from the canonical 2,4-dioxo tautomer was the kinetically and thermodynamically most favorable intermediate.[10] However, gas-phase investigations of cytosine radicals are complicated by the fact that the parent compound exists as a mixture of three major isomers, e.g., 2-oxo-4-amino-1,2-dihydro(*1H*)pyrimidine (**1**) and the syn- and anti-OH rotamers of 2-hydroxy-4-aminopyrimidine (**2** and **3**), that are at prototropic equilibrium, as studied previously by experiment and theory.[13] Hence, cytosine can be expected to give rise to a number of isomeric hydrogen atom adducts that are difficult to distinguish experimentally.[14]

To shed some light on the properties of hydrogen atom adducts to cytosine and derivatives, we now report a computational study of relative and dissociation energies of several cytosine radicals. Also investigated are activation energies for H-atom additions to the C-2, O-2, N-3, C-5, and C-6 positions in cytosine tautomers and the N-3, C-5, and C-6 positions in 1-methylcytosine and cytosine−water complexes. The N-1-methyl substituent blocks tautomerization of cytosine, so that the canonical 1-methyl-2-oxo-4-amino-1,2-dihydro(*1H*)pyrimidine form is the most stable isomer[15] as it is in cytidine and DNA. Water molecules solvating cytosine have been shown to affect the tautomer relative stabilities,[16] and so it was also of interest to examine the effect of water molecules on the activation energies for H-atom addition.

The energetics of cytosine radicals have been addressed computationally by Sevilla and co-workers, who used Hartree−Fock level calculations to estimate the enthalpies of formation of a number of radical adducts.[17] More recently, Eriksson,[5] Barone,[18] Close,[6] and other groups[19] reported density functional theory (DFT) calculations of H-atom adducts to cytosine that

* To whom correspondence should be addressed. Tel: (206) 685-2041. Fax: (206) 685-3478. E-mail: turecek@chem.washington.edu.

10.1021/jp030698d CCC: $25.00
Published on Web 10/01/2003

were focused on spin densities and hyperfine coupling constants. The present study is focused on radical dissociations and H-atom additions. Because DFT calculations are not always reliable in providing accurate transition state energies for radical reactions,[20] we employ the B3-PMP2 scheme for all systems under study.[21] The B3-PMP2 scheme is based on simple averaging of B3LYP and spin-projected MP2 energies obtained with adequately large basis sets of triple ζ quality and furnished with multiple polarization and diffuse functions, e.g., 6-311++G-(2d,p) and 6-311++G(3df,2p). Systematic investigation of medium-size (10−50 atoms) radical systems has shown that this empirical scheme results in cancellation of small errors inherent to both B3LYP and MP2 formalisms and provides dissociation and transition state energies that compare favorably with those from correlated QCISD(T) and CCSD(T) calculations but can be performed at a fraction of computational cost.[9,10,22] The theoretical background for the B3-MP2 scheme can be found in a study by Rassolov, Ratner, and Pople who showed that MP2 and B3LYP calculations underestimate and overestimate, respectively, the correlation energy in the bond dissociation in H_2.[23]

Calculations

Standard ab initio and density functional theory calculations were performed with the Gaussian 98 suite of programs.[24] Optimized geometries were obtained with density functional theory calculations using Becke's hybrid functional, B3LYP[25] and the 6-31+G(d,p) basis set. Harmonic frequencies were calculated to characterize stationary states as local minima (all real frequencies) and first-order saddle points (one imaginary frequency). Complete optimized geometries and harmonic frequencies can be obtained from the corresponding author upon request. The B3LYP/6-31+G(d,p) moments of inertia and harmonic frequencies were also used to calculate rotational and vibrational partition functions, enthalpies, and entropies using standard formulas of statistical thermodynamics. Single-point energies were obtained with B3LYP and Møller−Plesset perturbational calculations[26] truncated at second order, MP2, with frozen core and valence electron only excitations with the larger 6-311++G(3df,2p) basis set. Spin contamination in calculations with spin unrestricted wave functions was negligible to moderate, as judged from the $\langle S^2 \rangle$ operator expectation values that were 0.75−0.76 for UB3LYP calculations of local minima and transition states, 0.75−0.77 for UMP2 calculations of local minima, and 0.76−0.96 for UMP2 calculations of transition states. Spin projection[27] in MP2 single-point calculations (PMP2) reduced the $\langle S^2 \rangle$ values to 0.75−0.77 and resulted in energy corrections of 3 millihartree (8 kJ mol^{-1}) calculated as root-mean-square deviation. The single-point energies from the B3LYP and spin-projected MP2 calculations were averaged and used to calculate B3-PMP2 relative energies that were corrected for zero-point vibrational energies and are discussed throughout. This empirical procedure[21] has been shown to result in efficient cancellation of small errors inherent to B3LYP and MP2 formalisms and to provide relative and activation energies that in accuracy compare favorably with those from high level composite Gaussian 2 or Gaussian 2(MP2) calculations, as reported for several systems.[22] For selected cytosine radicals and transition states, single-point energies were also calculated according to a composite procedure that used coupled clusters calculations[28] with single, double, and perturbational triple excitations and the 6-31G(d,p) basis set. Basis set expansion to effective CCSD(T)/6-311++G(3df,2p) energies was accomplished using the linear formula E[CCSD(T)/6-311++G(3df,-2p)] ≈ E[CCSD(T)/6-31G(d,p)] + E[PMP2/6-311++G(3df,2p)] − E[PMP2/6-31G(d,p)]. Rate constants were calculated using the standard transition theory formula.[29] Activation energies were obtained by B3-MP2/6-311++G(3df,2p) calculations. Rotational and vibrational partition functions were calculated from B3LYP/6-31+G(d,p) moments of inertia and scaled harmonic frequencies. Tunneling corrections to the calculated rate constants were not considered. Solvation free energies were calculated by B3LYP/6-31+G(d,p) using the polarizable continuum model (PCM).[30] Structures were reoptimized by PCM-B3LYP/6-31+G(d,p) using standard parameters (water dielectric constant, atomic, and van der Waals radii) included in Gaussian 98.[24,30]

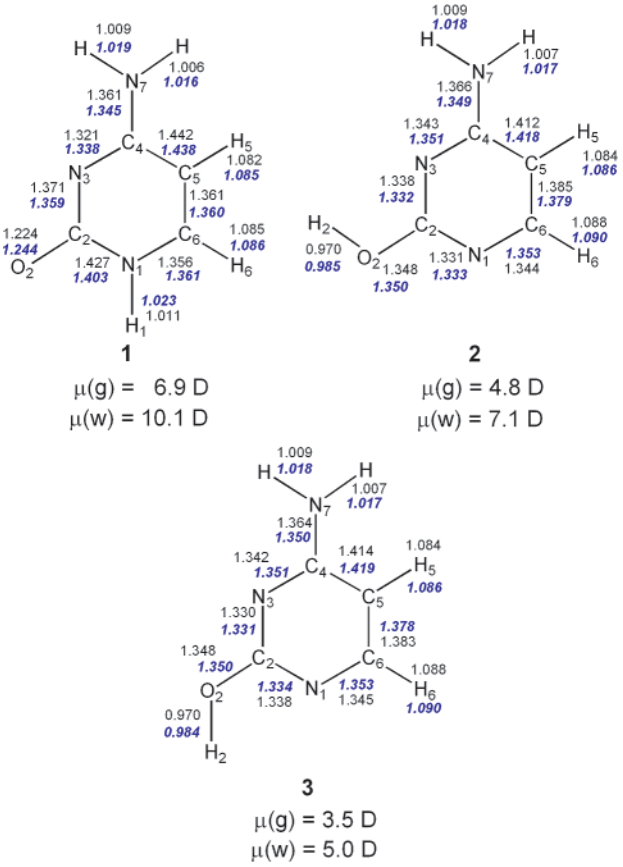

Figure 1. B3LYP/6-31+G(d,p) optimized structures of cytosine isomers **1**−**3**. Bond lengths (angstroms): black numerals refer to the isolated molecules in the gas phase, blue italics refer to molecules in a polarizable continuum with the dielectric constant of water. The dipole moments in units of Debye are for fully optimized structures and refer to the gas phase (μ(g)) or aqueous solution (μ(w)).

Results and Discussion

Gas-Phase Radical Structures and Relative Energies. Hydrogen atom additions were investigated for the three most stable cytosine isomers, e.g., 2-oxo-4-amino-1,2-dihydro(*1H*)-pyrimidine (**1**, Figure 1) and the OH rotamers of 2-hydroxy-4-aminopyrimidine (**2** and **3**, Figure 1). The relative stabilities of **1**−**3** in the gas phase have been addressed previously at high levels of ab initio theory by Kobayashi[13b] and Trygubenko et al.[16a] Structure **3** is the most stable isomer, whereas **1** and **2** are respectively 5.2−6.0 and 2.7−2.9 kJ mol^{-1} less stable than **3** at 0 K. Our effective CCSD(T)/6-311++G(3df,2p) energies with zero-point corrections give the relative 0 K energies in kJ mol^{-1} as 2.2 (**1**), 2.9 (**2**), and 0.0 (**3**). Hydrogen atom addition to **1** gives radicals **4**, **5, 6, 13, 14**, and **15** as local energy minima

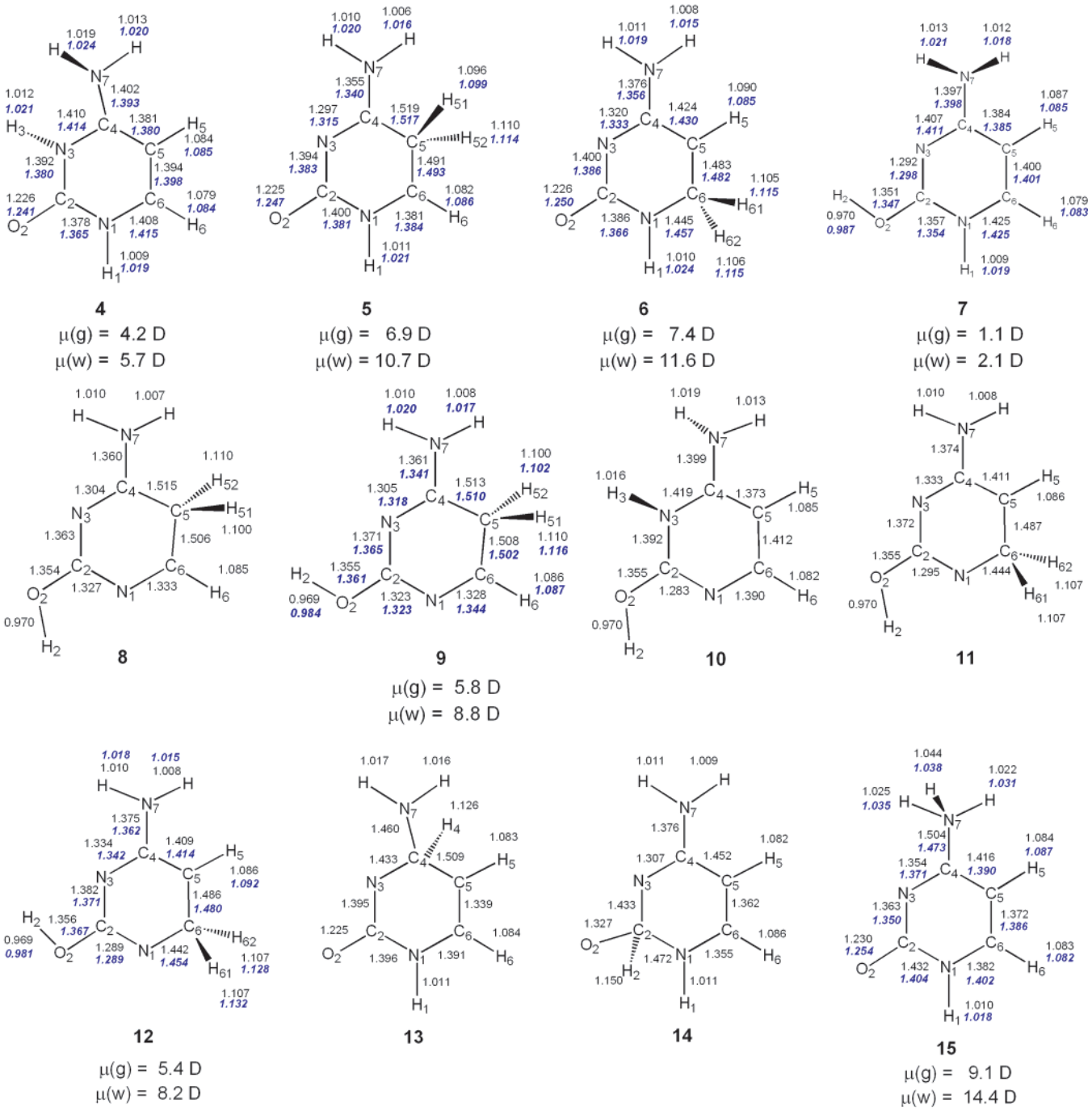

Figure 2. B3LYP/6-31+G(d,p) optimized structures of cytosine radicals **4**−**15**. Parameters as in Figure 1.

(Figure 2). The N-3 adduct **4** is the most stable structure in the gas phase, followed by the C-5 and C-6 adducts, **5** and **6**, respectively (Table 1). Some structure features of **4**−**6** deserve a brief comment. The rings in **4** and **6** are essentially planar, whereas the amino groups are pyramidal. In **4**, the amine hydrogen atom pointing toward N-3 is rotated 61° out of plane to avoid repulsive interaction with the N-3 hydrogen atom. The latter is 15° out of plane because of a slight pyramidization at N-3. The ring in **5** is puckered into a half-chair conformation with out-of plane C-5 and C-6 and the C-4-C-5-C-6-N-1 dihedral being equal to 32°. The optimized structures of **4**−**6** and the ordering of B3-PMP2 relative energies are consistent with the results of previous DFT calculations.[5,19]

The adducts to C-4, C-2, and the amino group (**13**, **14**, and **15**, respectively, Figure 2) are substantially less stable than **4** (Table 1). Structure **13** is an N-3-amidyl radical in which the hydrogen atom at C-4 disrupts conjugation with the exocyclic amino group. Structure **14** can be viewed as an alkoxy radical in which the H-atom at C-2 disrupts conjugation of the carbonyl group with the ring azadiene system. The H-atom adduct to the amino group (**15**) is a high-energy zwitterion consisting of a positively charged ammonium group and a negatively charged anion-radical ring, analogous to a hydrogen atom adduct to 4-aminopyrimidine.[11c] This description is supported by the atomic charges and spin densities calculated by Mulliken population analysis[31] that shows substantial polarization between the ammonium group (+0.66 total charge) and the ring (−0.66 total charge), with 93% of the spin density being delocalized among the N-1, N-3, C-4, and C-6 ring atoms. Also notable is the long N-7−C-4 bond (1.504 Å) and pyramidization at C-4

TABLE 1: Relative Energies of Cytosine Radicals

	relative energy[a]					
	B3LYP 6-31+G(d,p)	B3-MP2[b] 6-311++G(3df,2p)				CCSD(T)[c] 6-311++G(3df,2p)
radical	ΔH_0(g)[d]	ΔH_0(g)[d]	ΔH_{298}(g)[e]	ΔG_{298}(g)[f]	ΔG_{298}(w)[g]	ΔH_0(g)[d]
4	0	0	0	0	0	0
5	31	36	35	34	7	31
6	37	44	43	39	-1	43
7	54	51	51	53	59	
8	49	52				
9	46	56	56	60	48	
10	61	60				
11	66	71				
12	70	75	74	76	60	
13	142	155				
14	177	203				
15	162	162	161	162	78	

[a] In units of kJ mol^{-1}. All relative energies include ZPVE corrections. [b] From spin-projected MP2 energies. [c] From a linear extrapolation: E[CCSD(T)/6-311++G(3df,2p)] ≈ E[CCSD(T)/6-31G(d,p)] + E[PMP2/6-311++G(3df,2p)] − E[PMP2/6-31G(d,p)]. [d] Gas-phase relative enthalpies at 0 K. [e] Gas-phase relative enthalpies at 298 K. [f] Gas-phase relative free energies at 298 K. [g] Relative free energies in water.

which places the N-7 ammonium group 30° out of the ring plane. Radical **15** is 162 kJ mol^{-1} less stable than **4** (Table 1).

H-atom additions to the ring positions in **2** and **3** produce radicals **7**, **8**, **9**, **10**, **11**, and **12** as local energy minima (Figure 2, Table 1). The C-5 adducts (**8** and **9** differing in the orientation of the OH group) and the N-1 and N-3 adducts (**7** and **10**, respectively) have essentially planar rings. The H-1 hydrogen atom in **7** is slightly out of plane (8°) due to pyramidization at N-1, as is H-3 in **10** (30°) due to pyramidization at N-3. The amino group in **10** is twisted 56° out of plane to avoid an H···H repulsive interaction with H-3. The rings in **8** and **9** are slightly puckered into half-chair conformations with the C-4−C-5−C-6−N-1 dihedrals equal to 19 and 18°, respectively. Radicals **7**, **8**, and **9** are the most stable species of this group, which however are 51−56 kJ mol^{-1} less stable than **4**. The C-6 adducts **11** and **12** are yet 20 kJ mol^{-1} less stable (Table 1).

The isomeric radicals derived from 1-methylcytosine (**16**), e.g., the N-3 adduct **17**, and the C-5 and C-6 adducts, **18** and **19**, respectively, show structural features (Figure 3) and relative energies that are closely analogous to those of **4**−**6** (Table 2). The electron-donating methyl group in **17**−**19** causes a slight decrease in the dipole moments in the gas-phase structures when compared to **4**−**6**. However, this is compensated by the increased polarizability of **17**−**19** in water, so that the dipole moments calculated by PCM (Figure 3) are virtually identical to those for **4**−**6** (Figure 2).

Radical Structures and Relative Energies in Aqueous Solution. Geometry optimizations using PCM resulted in structure changes and provided free energies of solvation (ΔG_{solv}) for **4**−**6**, **9**, **12**, **15**, and **17**−**19** (Table 3). The other cytosine radicals were not investigated further. The differences between the structures optimized with B3LYP/6-31+G(d,p) for isolated species in the gas phase and using PCM were minor indeed, as all bond lengths differed by less than 0.02 Å between the gas-phase and solvated structures for cytosine isomers **1**−**3** (Figure 1), as well as for the radicals (Figure 2). More substantial differences ensued from the calculated solvation free energies (Table 3). With cytosine isomers, the 2-oxo form **1** is 22−25 kJ mol^{-1} more strongly solvated in water than the 2-hydroxy forms **2** and **3**, which reverses the gas phase ordering of relative free energies[13a] and renders **1** the most stable isomer in aqueous solution. Out of the radicals derived from **1**, structures **5** and **6** are more effectively solvated than **4**, so that the free energies for these three tautomers become very close in solution (Table 1). The highly polarized radical **15** has the highest solvation free energy in this group, but the free energy decrease upon solvation is insufficient to compensate the large free energy of gas-phase **15** relative to **4**, so that the former remains disfavored by 79 kJ mol^{-1} in solution. The less effective solvation of the 2-hydroxy group (vide supra) is retained in radicals **9** and **12** which are calculated to be substantially less stable than **4**−**6** in aqueous solution.

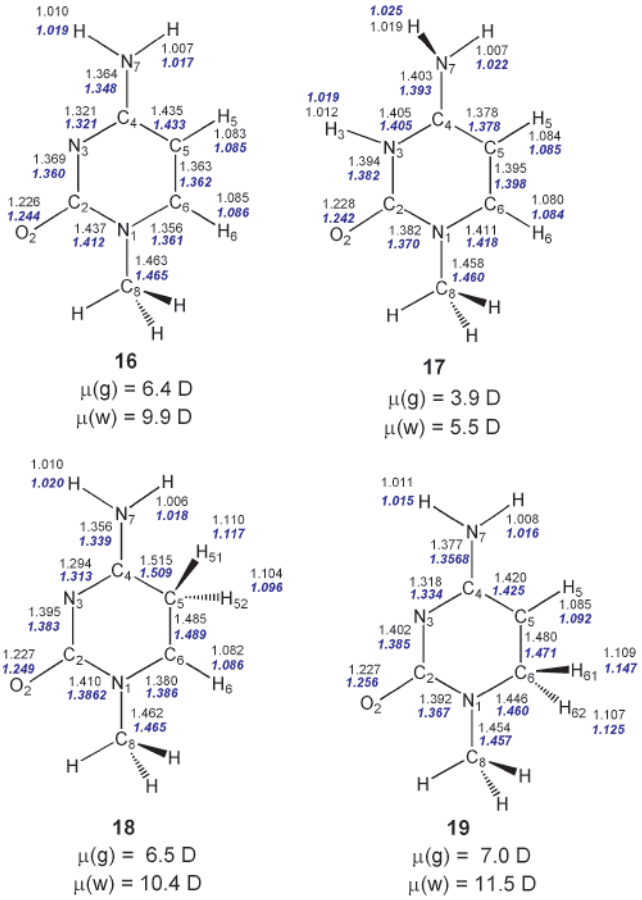

Figure 3. B3LYP/6-31+G(d,p) optimized structures of 1-methylcytosine (**16**) and radicals **17**−**19**. Parameters as in Figure 1.

The different solvation free energies of cytosine molecules and radicals can be related to their dipole moments. Figure 1 shows that, out of the three most stable cytosine isomers, **1** has the largest dipole moment (6.9 D) which further increases to 10.1 D in water. Hydrogen atom attachment to N-3 decreases

TABLE 2: Relative Energies of 1-Methylcytosine Radicals

	relative energy[a]				
	B3LYP	B3-MP2[b]			
radical	ΔH_0(g)[c]	ΔH_0(g)[c]	ΔH_{298}(g)[d]	ΔG_{298}(g)[e]	ΔG_{298}(w)[f]
16	0	0	0	0	0
17	31	36	35	32	5
18	38	43	43	40	0.5

[a] In units of kJ mol-1. All relative energies include ZPVE corrections. [b] From spin-projected MP2 energies with the 6-311++G(3df,2p) basis set. [c] Gas-phase relative enthalpies at 0 K. [d] Gas-phase relative enthalpies at 298 K. [e] Gas-phase relative free energies at 298 K. [f] Relative free energies in water.

TABLE 3: Solvation Free Enthalpies

species	$\Delta G_{298,solv}$[a,b]	$\Delta G_{298,solv}$[a,c]
1	−81	−90
2	−62	−68
3	−59	−64
4	−67	−70
5	−88	−97
6	−98	−111
7	−59	−64
9	−91	−86
12	−80	−82
15	−131	−153
16	−70	−83
17	−56	−59
18	−88	−86
19	−102	−99

[a] PCM calculations with the 6-31+G(d,p) basis set using standard parameters and the dielectric constant of water; free energies in units of kJ mol^{-1}. [b] Solvation free enthalpies for structures optimized by B3LYP/6-31+G(d,p) in the gas phase and solvated in water. [c] Solvation free enthalpies for structures optimized by PCM-B3LYP/6-31+G(d,p) in the water dielectric.

both the dipole moment of gas-phase **4** and its polarizability, so that the dipole moment is only 5.7 D in water (Figure 2). This effect is most likely due to the parallel arrangement of the H-3(+)−N-3(−) and O-2(−)−C-2(+) bond dipoles that decrease the total dipole moment of **4**. Hydrogen atom attachment to C-5 and C-6 has only a small effect on the dipole moment in **5** and **6** when compared to that in **1**. Of these, **6** shows a greater dipole moment which, according to the atomic charges, can be assigned to polarization of theO-2(−)−C-2−N-3−C-4−C-5(+) conjugated π-bond system, further increasing in water (Figure 2).

The radicals produced by hydrogen atom addition to **16** (**17**−**19**) show a behavior that is entirely analogous to that of **4**−**6** and need not be discussed in detail. The optimized structures of **16**, and **17**−**19** are shown in Figure 3.

Cytosine−**Water Complexes.** In addition to investigating the effect of bulk solvent polarization on the cytosine radical structures and relative energies, we also addressed the question of specific interactions between the cytosine moiety and water molecules when the latter were hydrogen bonded to N-1, N-3, and N-7 or the corresponding nitrogen bound protons. For **1** we found two 1:1 water adducts in which the water molecule was hydrogen bonded to N-1, O-2 (**20**), or N-3, N-7 (**21**). A 2:1 water adduct (**22**) was also found to be a local energy minimum. The optimized structure of **20** (Figure 4) shows that the water molecule is bound by two hydrogen bonds, one between the water oxygen and H-1 (1.947 Å) and the other between one of the water hydrogens and O-2 (1.815 Å). Water bonding has a negligible effect on the bond lengths in the remote part of the molecule, as shown by comparing the structures of **20**−**22** (Figure 4) with that for **1** (Figure 1), but results in the expected lengthening of the C-2−O-2 and N-1−H-1 bonds in **20** compared to those in **1**. In the isomeric 1:1 complex **21**, the water molecule has one hydrogen bond between its oxygen and the syn-oriented amine hydrogen and the other between N-3 and one of the water protons. These features are combined in complex **22** that binds two water molecules (Figure 4).

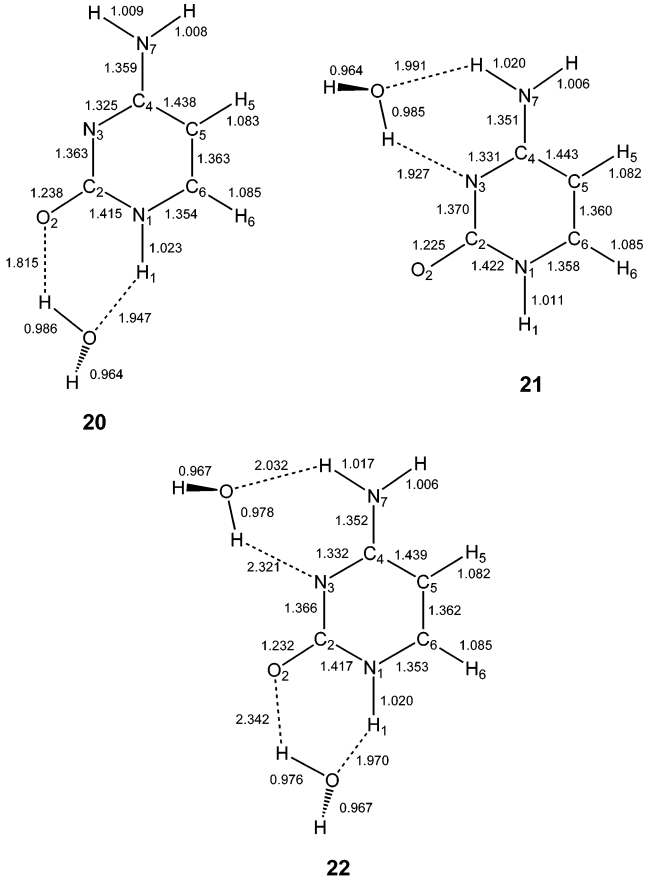

Figure 4. B3LYP/6-31+G(d,p) optimized structures of cytosine-water complexes **20**−**22**.

TABLE 4: Dissociation Enthalpies and Free Energies of Cytosine-Water Complexes in the Gas Phase

	energy[a,b]	
reaction	ΔH_{298}(g)	ΔG_{298}(g)
20 → **1** + H_2O	45	12
21 → **1** + H_2O	42	6
22 → **20** + H_2O	38	-2.5
22 → **21** + H_2O	41	4
23 → **4** + H_2O	34	−3
24 → **5** + H_2O	36	−1
25 → **6** + H_2O	37	−2
26 → **4** + H_2O	18	−8
27 → **5** + H_2O	39	0.4
28 → **6** + H_2O	39	8.5
29 → **4** + $2H_2O$	51	−12
30 → **5** + $2H_2O$	73	−2
31 → **6** + $2H_2O$	67	−8.5

[a] In units of kJ mol^{-1}. [b] From B3−PMP2/6-311++G(3df,2p) relative energies and B3LYP/6 31+G(d,p) zero-point vibrational energy corrections, enthalpies, and entropies.

The dissociation enthalpies and free energies for **20**−**22** are shown in Table 4. The bonding energies for the water molecule are similar in **20** (45 kJ mol^{-1}) and **21** (42 kJ mol^{-1}) and result in positive free energies for dissociation for both complexes which are calculated to be bound at 298 K. In contrast, the second water molecule is bound less strongly (ΔH_{298} = 38 kJ

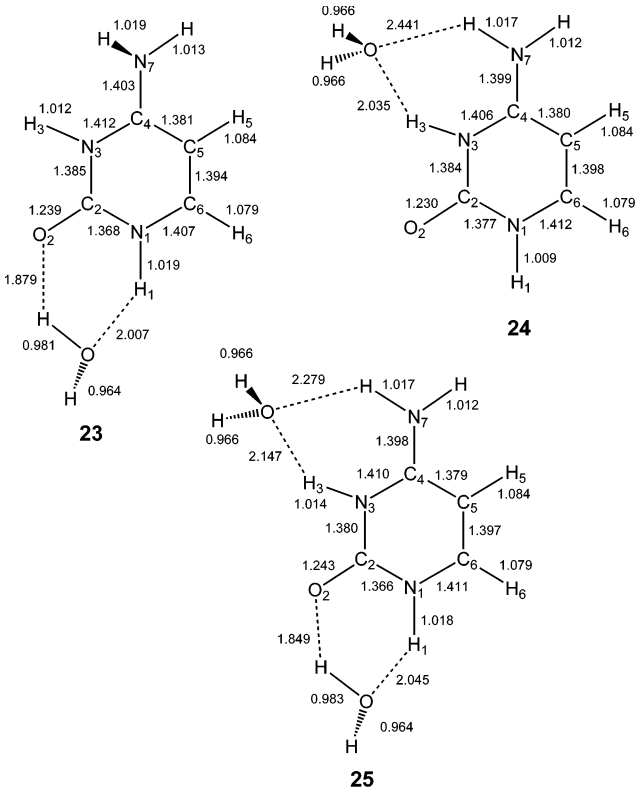

Figure 5. B3LYP/6-31+G(d,p) optimized structures of cytosine-water radicals **23**−**25**.

mol^{-1}), so that **22** is predicted to dissociate exoergically to **20** and water, ΔG_{298}(**22** → **20**) = −2.5 kJ mol^{-1}.

Hydrogen bonding of water molecules in radicals **4**−**6** is in general weaker than in **1** and depends on the site where the hydrogen atom is attached to. Radical complexes **23**−**25** bind water at N-1 and O-2 (Figure 5) with binding enthalpies in the 34−37 kJ mol^{-1} range (Table 4). However, the entropy gain upon dissociation results in negative free energies that indicate that the complexes are unbound at 298 K.

A substantial difference in water binding energies is calculated for radical complexes **26**−**28** (Figure 6, Table 4). In **26**, the ring hydrogen (H-3) prevents the protons of the water molecule from hydrogen bonding to N-3. Instead, the water oxygen forms hydrogen bonds to H-3 and the syn-oriented exocyclic amine hydrogen atom. This arrangement results in substantially longer hydrogen bonds in **26** than in **27** and **28** where the steric hindrance due to H-3 is absent (Figure 6). As a consequence, the water binding energy in **26** is substantially smaller (18 kJ mol^{-1}) than in the other radicals, and the 298 K free energy for water loss is negative, indicating that the complex will dissociate spontaneously at room temperature (Table 4). Complex **27** is marginally bound at 298 K, whereas **28** is predicted to be thermodynamically stable.

The 2:1 water radical complexes **29**−**31** combine the structure features described for the 1:1 complexes **23**−**25** and **26**−**28** (Figure 7). The second water molecule is only weakly bound (Table 4), and the negative free energies for water loss indicate facile dissociation to the corresponding 1:1 complexes (e.g., **31**), or complete dissociation to form cytosine radicals **4** and **5**.

Reaction Enthalpies and Transition States for Hydrogen Atom Additon to Cytosine. In this section, we will first describe the calculated trends in the reaction and transition state energies for H-atom additions to cytosine and 1-methylcytosine in the gas phase and compare those to analogous reactions in

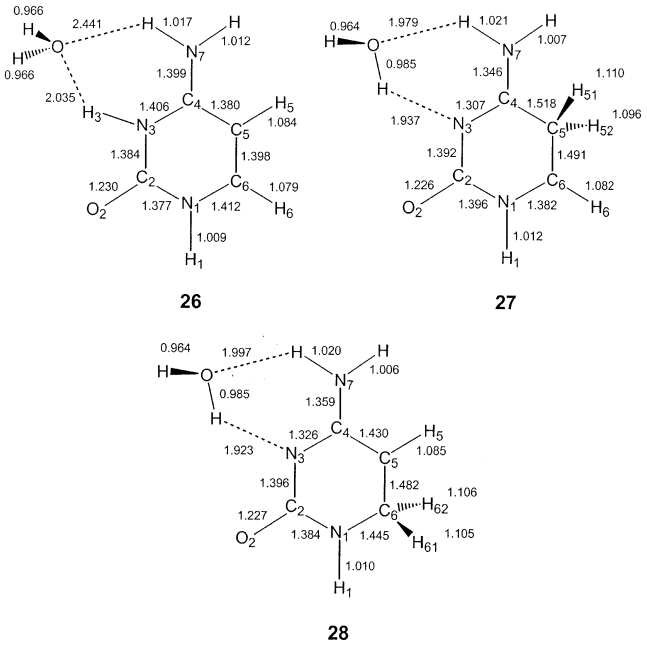

Figure 6. B3LYP/6-31+G(d,p) optimized structures of cytosine-water radicals **26**−**28**.

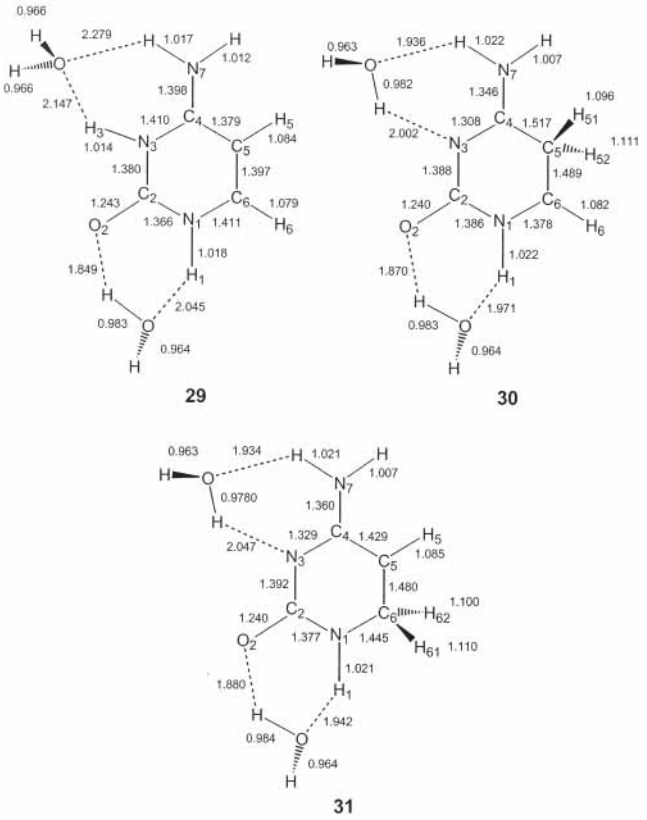

Figure 7. B3LYP/6-31+G(d,p) optimized structures of cytosine-water radicals **29**−**31**.

water and in water-complexes **20**−**22**. The electronic effects that can be used to interpret the data will be discussed next.

Hydrogen atom addition to cytosine tautomer **1** is an exothermic reaction if occurring in positions N-3, C-5, and C-6, whereas additions to C-2, C-4, and the amino group are endothermic (Table 5). Hence, positions N-3, C-5, and C-6 are the most favorable candidates for a radical attack and were the focus of our kinetic and solvation studies. Solvation effects on the thermochemistry of H-atom addition were investigated both

TABLE 5: Reaction Energies for Hydrogen Atom Additions

reaction	energy[a] B3-PMP2[b]	CCSD(T)[c]
1 + H → **4**	−131 (−106)[d] (−72)[e]	−130
1 + H → **5**	−95 (−71)[d] (−64)[e]	−98
1 + H → **6**	−87 (−66)[d] (−73)[e]	−87
2 + H → **7**	−84	
3 + H → **8**	−80	
2 + H → **9**	−79	
3 + H → **10**	−72	
16 + H → **17**	−128 (−104)[d] (−66)[e]	
16 + H → **18**	−92 (−71)[d] (−60)[e]	
16 + H → **19**	−84 (−63)[d] (−65)[e]	
20 + H → **23**	−123 (−127)[d]	
20 + H → **24**	−89 (−94)[d]	
20 + H → **25**	−83 (−88)[d]	
21 + H → **26**	−114 (−115)[d]	
21 + H → **27**	−95 (−100)[d]	
21 + H → **28**	−89 (−92)[d]	
22 + H → **29**	−106 (−107)[d]	
22 + H → **30**	−88 (−93)[d]	
22 + H → **31**	−74 (−78)[d]	

[a] In units of kJ mol^{-1}. All energies include zero-point corrections and refer to 0 K unless stated otherwise. [b] From averaged B3LYP and spin-projected MP2 single-point energies. [c] From a linear extrapolation: E[CCSD(T)/6-311++G(3df,2p)] ≈ E[CCSD(T)/6-31G(d,p)] + E[PMP2/6-311++G(3df,2p)] − E[PMP2/6-31G(d,p)]. [d] 298 K reaction free energies in the gas phase. [e] 298 K reaction free energies in aqueous solution.

using the PCM model and calculating the reaction enthalpies and free energies for the cytosine−water complexes **20**−**22**. The hydration free energy of the hydrogen atom was taken as 13.5 kJ mol^{-1} from the work of Gai and Garrett.[32]

The gas-phase data show that H-atom addition to cytosine is affected by the presence of water molecules that are hydrogen-bonded to the nucleobase. For addition to N-3, the water molecules destabilize the radical adducts by 8, 17, and 25 kJ mol^{-1} for **23**, **26**, and **29**, respectively. This destabilization appears to be a cumulative effect. H-atom additions to C-5 and C-6 are affected differently by water complexation. In **20**, where the water molecule is hydrogen bonded to H-1 and O-2, H-atom addition to C-5 and C-6 is 6 and 5 kJ mol^{-1} less exothermic, respectively, than in **1**, indicating again that water complexation destabilizes the radicals. In contrast, water complexation in **21** has no effect on H-atom addition to C-5 and a small stabilizing effect on addition to C-6 (Table 5). In the presence of two water molecules (**22**), H-atom addition to C-5 and C-6 is again disfavored by 7 and 13 kJ mol^{-1}, respectively, relative to the corresponding additions to **1**.

The effect of bulk water differs for H-atom additions to N-3, C-5, and C-6 (Table 5). Although the reaction free energies decrease substantially for addition to N-3 (from −106 kJ mol^{-1} in the gas phase to −72 kJ mol^{-1} in bulk water), and less so for addition to C-5 (from −71 to −64 kJ mol^{-1}), addition to C-6 is more exothermic in bulk water (−73 kJ mol^{-1}) than in the gas-phase (−66 kJ mol^{-1}). This shows that the radical stabilities are greatly affected by solvent effects.

Hydrogen atom additions to 1-methylcytosine (**16**) show a trend which is entirely similar to that described for **1**. The effect of the *N*-methyl group is to slightly decrease the addition exothermicity in both the gas phase and bulk water (Table 5).

More important than the reaction thermodynamics are the activation energies for H-atom addition and the effect of environment on the reaction kinetics. The calculated activation energies for H-atom additions to **1**, **2**, **3**, **16**, and water complexes **20**−**22** are summarized in Table 6. The representative

TABLE 6: Activation Energies and Rate Constants for H-Atom Additions to Cytosine, 1-Methylcytosine, and Cytosine−Water Complexes

		B3-PMP2 energies				CCSD(T) energies			
reactant	position	E_a[a]	E_{Arrh}[b]	log A	log k_{298}[c]	E_a[a]	E_{Arrh}[b]	log A	log k_{298}[c]
1	C-5	13.5	13.5	12.70	10.32	18.8	18.9	12.70	9.39
	N-3	17.6	17.4	12.61	9.56	24.4	24.2	12.61	8.36
	C-6	22.7	22.9	12.78	8.76	29.5	29.7	12.78	7.58
	O-2	40.5	40.9	12.89	5.72				
2	C-5	14.3	14.6	12.86	10.30				
	C-6	25.0	25.4	12.88	8.42				
	N-1	27.4	27.6	12.78	7.95				
3	C-5	14.5	14.7	12.82	10.24	22.5	22.7	12.82	8.84
	N-3	23.5	23.2	12.64	8.56	32.8	32.5	12.64	6.93
	C-6	25.0	25.4	12.86	8.41	34.2	34.5	12.86	6.81
16	C-5	12.2	12.3	12.70	10.55				
	N-3	17.0	17.1	12.72	9.73				
	C-6	20.8	21.2	12.90	9.19				
20	C-5	15.0	14.5	12.11	9.57				
	N-3	19.5	18.8	12.03	8.74				
	C-6	24.0	23.7	12.25	8.10				
21	C-5	14.9	15.1	12.77	10.12				
	N-3	27.4	27.7	12.97	8.12				
	C-6	23.9	24.2	12.85	8.61				
22	C-5	15.2	15.9	13.03	10.24				
	N-3	28.2	28.6	13.07	8.05				
	C-6	24.0	24.5	12.95	8.65				

[a] Activation energies for H atom additions in units of kJ mol^{-1}. [b] Arrhenius activation energies. [c] 298 K bimolecular rate constants in mol^{-1} cm^3 s^{-1}.

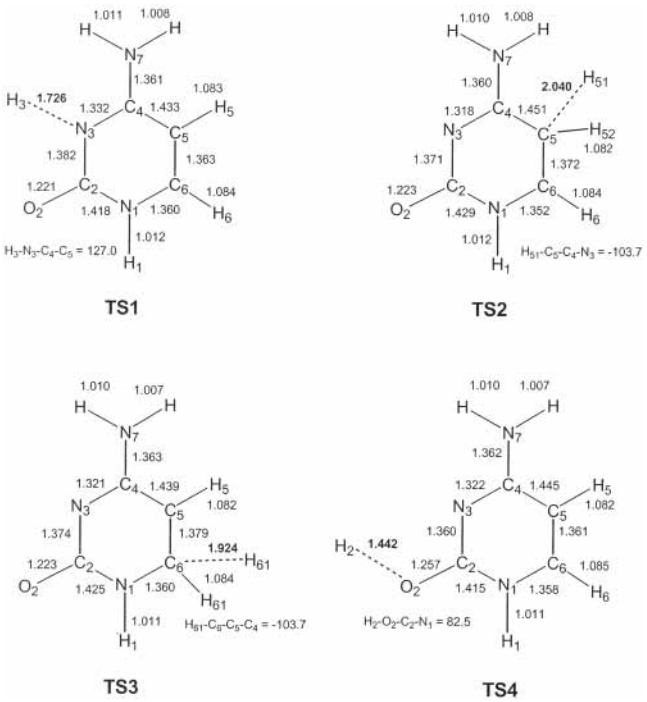

Figure 8. B3LYP/6-31+G(d,p) optimized structures of transition states for hydrogen atom additions in **1**.

transition state structures for additions to **1** and **21** are shown in Figure 8 (**TS1**−**TS4**) and Figure 9 (**TS18**−**TS20**), those for additions to **2**, **3**, **16**, **20**, and **22** are given as Supporting Information (**TS5**−**TS17**, **TS21**−**TS23** Tables S36−S54). The TS for addition to N-3 in **1** (**TS1**, Figure 8) shows the H-atom approaching N-3 at a distance of 1.726 Å and out of the ring plane. The TS for additions to C-5 (**TS2**) and C-6 (**TS3**) also show out-of-plane approach of the H-atom and C···H distances of 2.040 and 1.924 Å, respectively.

The ordering of the activation energies (E_a) for H-atom addition to **1** indicates that C-5 is the most reactive position,

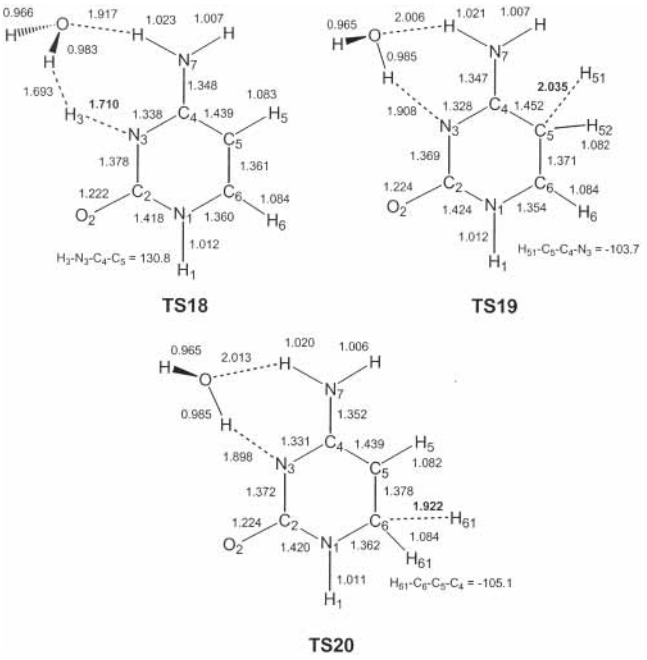

Figure 9. B3LYP/6-31+G(d,p) optimized structures of transition states for hydrogen atom additions in **21**.

followed by N-3 and C-6 (Table 6). Additions to O-2 and C-2 have substantially higher activation energies and are predicted to be disfavored. The same ordering of activation energies is obtained for H-atom additions to **16** which show overall slightly lower E_a values for all three of the most reactive positions. It may be noted that the B3-PMP2 scheme gives the same ordering of activation energies as do the much more expensive effective CCSD(T)/6-311++G(3df,2p) calculations, although the E_a data from the latter are offset up by 6.3 ± 0.9 kJ mol^{-1} (Table 6). C-5 is also calculated to be the most reactive position in cytosine isomers **2** and **3** in the gas phase, with activation energies being similar to that for addition to **1**. The other reactive positions in **2** and **3** are C-6 and the ring nitrogen atoms. In **2**, an H-atom addition to N-3 would result in the formation of an unstable syn-OH rotamer of **10** and likely does not occur. H-atom addition to the position N-1 shows slightly higher E_a than does addition to C-6. In **3**, addition to N-3 is more favorable than addition to C-6, although both have substantially higher activation energies than the addition to C-5 (Table 6).

Solvation effects on the ordering of activation energies for H-atom additions were studied for cytosine-water complexes **20**−**22**. In **20**, the activation energies follow the same trend as in **1** and **16** in that C-5 is the most reactive position followed by N-3 and C-6. Overall, water complexation in **20** slightly increases the E_a for all three additions and results in diminished reactivity. In contrast, water complexation in **21** primarily affects addition to N-3 which shows a substantially greater E_a relative to **20**, whereas the E_a for additions to C-5 and C-6 are virtually unaffected. The effect on E_a of the second water molecule in **22** is very weak and concerns mainly addition to N-3 which shows a yet higher activation energy. Thus, water complexation in **21** and **22** results in a *reversal of relative reactivities of N-3 and C-6* by disfavoring the addition to N-3.

PCM calculations of solvation free energies for transition states of H-atom addition did not give reasonable results. This is probably due to the PCM setup, where hydrogen atoms are included in the atomic radii of heavy atoms (X), and the structures are presumed to have standard X−H bond lengths.[30] This principle is violated in transition states for H addition, where the X−H bonds are 50−70% longer than the standard bonds and the model fails.

Electronic Effects on Hydrogen Atom Additions. The H-atom additions show some common features but also differences that are now discussed using orbital analysis and electron distributions calculated from Mulliken populations[31] of the reactants and transition states. The features that are common to H-atom additions to the N-3, C-5, and C-6 positions in **1**, **3**, **16**, and **20**−**22** are that (1) all these reactions are exothermic and (2) they all involve modest activation energies which are in a 13−28 kJ mol^{-1} range. The activation energies do not correlate with the reaction exothermicities,[11c] as the most stable N-3 adducts require higher activation energies for H-atom addition than do the less stable C-5 adducts. The electron donating 1-methyl group in **16** slightly lowers the TS energies for all H-atom additions, whereas hydrogen bonding to water in **20**−**22** causes the TS energies to increase (Table 6).

A hydrogen atom addition to cytosine or its derivatives involves an unpaired electron in the low-energy hydrogen atom 1s orbital ($-\epsilon$ = 13.59 eV) which interacts with electrons in the cytosine frontier orbitals to produce an electron pair occupying a low-energy σ-bonding orbital of the newly formed N−H or C−H bond, and an unpaired electron which occupies the highest (singly occupied) molecular orbital (SOMO) of the radical adduct. The extent of electron reorganization en route to products determines the activation energy of the reaction. Molecular orbital analysis of the frontier orbitals in **1**, **16**, and **20**−**22**, their radical products, and pertinent transition states showed, in general, very similar orbital shapes that can be represented by those for H-atom addition to **22** (Figure 10). The highest occupied molecular orbital (HOMO) in **22** is a π-type orbital shown in Figure 10. The TS for H-atom attack at C-5 (**TS22**) shows the SOMO as an antibonding combination of the hydrogen 1s orbital with the HOMO in **22**. The diminished expansion coefficients at C-2 and C-5 in **TS22** indicates a (39α + 40α) mixing with an unoccupied orbital in **22** which has an opposite phase at these carbon atoms. Likewise, the π-type SOMO for the transition state of H-atom addition at C-6 (**TS23**) can be viewed as arising from a combination of cytosine (39α + 40α) and hydrogen 1s orbitals. In contrast, the SOMO for addition to N-3 (**TS21**) involves a lower-lying (36α, $-\epsilon$ = 8.0 eV) orbital in **22** that has a strong component localized at N-3 (Figure 10).

The electron reorganization in the transition states for H-atom additions can be visualized by the total atomic charges and spin densities at the attacking H-atom and the cytosine ring atoms as shown for **1** (Table 7). In **TS1**, the H-atom addition causes electron density flow from N-3 to C-4 and C-5 which both show increased electron densities compared with those in **1**. The attacking H-atom retains most (77%) of the spin density and shows a negligible atomic charge. This is consistent with **TS1** being an early transition state. The charge polarization in the cytosine ring in **TS1** indicates that the H-atom attacking at N-3 can be viewed as a weak nucleophile. In **TS2**, the H-atom has a negligible charge and retains most (79%) of the spin density. The atomic charges indicate electron density flow to C-5 and C-4, so that the H-atom can be viewed as a weak nucleophile. In contrast, in **TS3**, the attacking H-atom develops a small positive charge and causes a polarization of the C-5−C-6 bond, whereby C-6 develops an increased negative atomic charge, whereas C-5 becomes more positive. Hence, the attacking H-atom in **TS3** can be viewed as a weak electrophile.

The electron reorganization trends during H-atom attack in positions N-3, C-5, and C-6 in **16** and **20**−**22** are analogous to

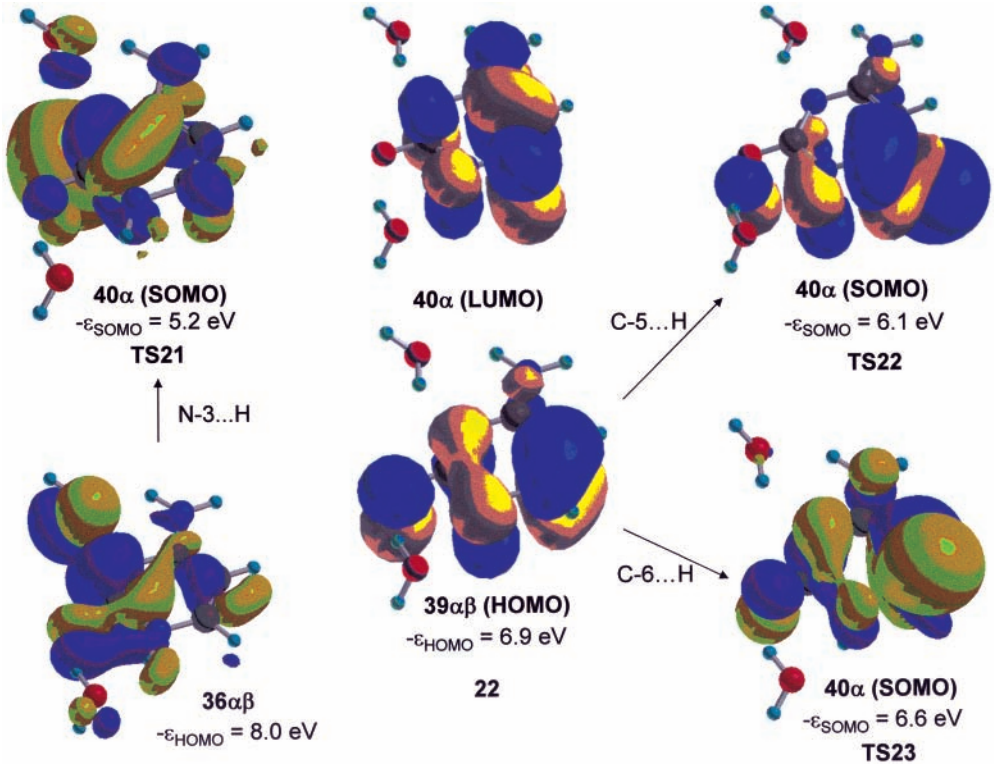

Figure 10. Molecular orbitals in **22** and **TS21-TS23**. The isosurface was set at 0.025.

TABLE 7: Atomic Charges and Spin Densities in Cytosine and Cytosine Radicals

	charge and spin densities[a]										
species	N-1	C-2	O-2	N-3	C-4	C-5	C-6	N-7	H-3	H-5	H-6
1	−0.41	0.55	−0.53	−0.48	0.25	0.12	−0.16	−0.55			
TS1	−0.40	0.57	−0.52	−0.35	0.20	−0.02	−0.19	−0.52	0.00		
	−0.01	0.04	0.01	−0.16	**0.16**	0.09	0.09	0.01	**0.77**		
4	−0.45	0.65	−0.54	−0.53	−0.02	0.28	−0.27	−0.62	0.32		
	0.06	−0.01	0.00	0.09	**0.44**	−0.24	**0.64**	0.06	0.00		
TS2	−0.39	0.55	−0.52	−0.45	0.12	0.09	−0.17	−0.51		0.01	
	0.02	0.00	0.03	−0.04	**0.24**	−0.30	**0.28**	−0.03		**0.79**	
5	−0.37	0.51	−0.51	−0.45	0.34	−0.22	−0.17	−0.54		0.16	
	0.07	0.00	0.09	0.00	0.01	−0.11	**0.90**	0.00		0.07	
TS3	−0.36	0.56	−0.52	−0.46	0.22	0.33	−0.53	−0.55			0.03
	−0.05	−0.03	0.00	0.07	0.01	0.08	**0.15**	0.02			**0.76**
6	−0.47	0.54	−0.51	−0.44	0.25	0.17	−0.39	−0.55			0.16
	0.03	−0.03	0.03	**0.30**	−0.17	**0.88**	−0.12	0.01			0.05
15	−0.42	0.57	−0.54	−0.60	0.05	−0.16	−0.07	−0.15		0.82[b]	
	0.13	0.02	0.01	**0.24**	**0.39**	−0.12	**0.30**	−0.12		**0.16**[b]	
21	−0.41	0.65	−0.53	−0.58	0.18	0.24	−0.24	−0.60			
TS18	−0.40	0.57	−0.52	−0.40	0.16	0.16	−0.23	−0.57	0.03		
	0.00	0.04	0.01	−0.11	**0.11**	0.07	0.06	0.01	**0.74**		
26	−0.44	0.72	−0.56	−0.53	−0.08	−0.32	−0.32	−0.63	0.37		
	0.06	0.00	0.00	0.09	**0.41**	−0.23	**0.66**	0.05	0.00		
TS19	−0.38	0.65	−0.52	−0.56	0.09	0.19	−0.25	−0.56		0.02	
	0.02	0.00	0.03	−0.03	**0.26**	−0.33	**0.29**	−0.03		**0.79**	
27	−0.37	0.60	−0.52	−0.54	0.321	−0.20	−0.18	−0.58		0.18	
	0.07	0.00	0.09	0.00	0.01	−0.11	**0.91**	0.00		0.07	
TS20	−0.35	0.66	−0.52	−0.57	0.16	0.43	−0.57	−0.59			0.03
	−0.05	−0.03	0.00	0.06	0.02	0.09	**0.14**	0.02			**0.76**
28	−0.46	0.65	−0.52	0.56	0.22	0.27	−0.45	−0.61			0.16
	0.02	−0.02	0.02	**0.25**	−0.17	**0.91**	−0.12	0.04			0.05

[a] From Mulliken population analysis. Upper lines: atomic charges on heavy atoms. Lower lines: spin densities on heavy atoms or hydrogen atoms, as denoted. Sites of major spin density are shown as bold numerals. [b] Sum of charge/spin densities on the ammonium hydrogen atoms.

that described for **1** and do not depend on the mode of water complexation. For example, the negative charge at N-3 decreases from −0.58 in **21** to −0.40 in **TS18**, whereas the positive charge at C-5 decreases from 0.24 to 0.16 (Table 7). The charge and spin density at the attacking H atom are −0.03 and 0.74, respectively, in **TS18**, which are not much different from those in **TS1**. Hence, neither the orbital analysis nor the charge and spin densities provide a straightforward explanation for the reactivity reversal of N-3 and C-6 in water complexes **21** and **22**. An explanation can be inferred from the bonding energies of the water molecule coordinated to N-3 and the NH_2 group. The bonding energy decreases from 40 kJ mol^{-1} (0 K value) in

21 to 26 kJ mol^{-1} in **TS18**, and further to 20 kJ mol^{-1} (0 K value) in radical **26**. In contrast, the water bonding energy in **TS20** is calculated as 35 kJ mol^{-1}, indicating a stronger solvation of the transition state for addition at C-6. Hence, the reversed order of reactivities at N-3 and C-6 in **21** and **22** can be attributed to solvation effects. Note that the water bonding energy in **TS19** is 34 kJ mol^{-1}, a 6 kJ mol^{-1} decrease when compared to **21**, which results in an increased activation energy for H-atom addition at C-5 (14.9 kJ mol^{-1} in **21** compared to 13.5 kJ mol^{-1} in **1**) but does not change the reactivity ordering.

Hydrogen Atom Addition Kinetics. The calculated activation energies for H-atom additions were further used for transition state theory calculations of bimolecular rate constants, as summarized in Table 6. The relative rate constants for additions to the N-3, C-5, and C-6 positions are mainly determined by the respective activation energies, as the preexponential factors are very similar for each given reactant, e.g., log $A = 12.61-12.89$ for additions to **1**, and likewise for the other cytosine isomers or derivatives. For gas-phase cytosine isomers, addition to C-5 is predicted to dominate. The branching ratios for the formation of radicals **4**−**12** can be estimated from the equilibrium populations of cytosine isomers and the topical rate constants. Presuming that H atoms are the limiting reagent and the cytosine isomer equilibrium does not change in the course of H-atom addition, the fractions of radicals R_{ij} can be expressed by eq 1, where k_{ij} are the topical rate

$$R_{ij} = \frac{\alpha_i k_{ij}}{\sum_{i,j} \alpha_i k_{ij}} \qquad (1)$$

constants for cytosine isomers and α_i are the isomer equilibrium molar fractions. The latter were calculated using Kobayashi's relative energies,[13b] B3LYP/6-31+G(d,p) zero-point corrections, and 298 K enthalpies and entropies as 14% (**1**), 21% (**2**), and 65% (**3**). According to eq 1, the C-5 adducts **8** and **9** total 81% of all products, followed by **5** (14%), **4** (2%), **10** (1%), and **11** and **12** (1% total). H-atom additions to **16** show similar branching ratios, e.g., 84% **18**, 12% **17**, and 4% **19**. The branching ratios for water adducts **21** and **22** show an even greater preference for C-5 additions and a reversed ordering of N-3 and C-6 additions, e.g., 96% **27**, 3% **28**, and 1% **26**. These figures can be extrapolated to predict the branching ratios for H-atom addition in aqueous solution, where cytosine predominantly exists as the oxo tautomer **1**.[15] Presuming that solvation in bulk water involves water molecules specifically hydrogen bonded to N-3 and the NH_2 group, the kinetics of H-atom addition should be similar to that in the model complexes **21** and **22**, so that addition to C-5 should predominate. This is consistent with experimental data from pulse radiolysis in solution which showed the C-5 adduct to be the major product.[3,4] The concurrent formation of other adducts, which is predicted to be very minor by our calculations, can be due to other mechanisms of radiation damage that do not involve H-atom attack, e.g., electron capture followed by protonation.[1,2]

Conclusions

Solvent effects play a major role in affecting the relative stabilities of radicals produced by hydrogen atom addition to cytosine and 1-methylcytosine. Although N-3 adducts are the most stable isomers in the gas phase, in bulk water, the N-3, C-5, and C-6 adducts are comparably stable because of different free energies of solvation. Kinetically, H-atom addition prefers attack at C-5 in all tautomers and water complexes. In the gas phase, N-3 is calculated to be the second most reactive position in the 2-oxo-4-amino-1,2-dihydro(*1H*)pyrimidine tautomer **1** and in 1-methyl-2-oxo-4-amino-1,2-dihydro(*1H*)pyrimidine (**16**), followed by C-6. However, a water molecule solvating the N-3 position and NH_2 group in cytosine hampers addition to N-3 and reverses the relative reactivities of the C-6 and N-3 positions.

Acknowledgment. Support of this work by the National Science Foundation (Grant CHE-0090930) is gratefully acknowledged. The Chemistry Computer Facility was jointly funded by the NSF-CRIF (CHE-9808182) and University of Washington.

Supporting Information Available: Tables S1−S54 with B3LYP/6-31+G(d,p) optimized geometries in Cartesian coordinate format. This material is available free of charge via the Internet at http//:pubs.acs.org.

References and Notes

(1) Von Sonntag, C. In *Physical and Chemical Mechanism in Molecular Radiation Biology*; Glass, W. A., Varma, M. N., Eds.; Plenum Press: New York, 1991; pp 287−321.

(2) Becker, D.; Sevilla, M. D. In *Advances in Radiation Biology*; Lett, J. T., Sinclair, W. K., Eds.; Academic Press: San Diego, 1993; Vol. 17, pp 121−180.

(3) (a) Holmes, D. E.; Ingalls, R. B.; Myers, L. S., Jr. *Int. J. Radiat. Biol.* **1967**, *13*, 225−243. (b) Westhof, E. *Int. J. Radiat. Biol.* **1973**, *24*, 389−400. (c) Westhof, E.; Hüttermann, J. *Int. J. Radiat. Biol.* **1973**, *24*, 627−630. (d) Westhof, E.; Flossmann, W.; Müller, A. *Int. J. Radiat Biol.* **1975**, *28*, 427−438. (e) Flossmann, W.; Westhof, E.; Müller, A. *Int. J. Radiat. Biol.* **1976**, *30*, 301−315. (f) Hole, E. O.; Nelson, W. H.; Sagstuen, E.; Close, D. *M. Radiat. Res.* **1998**, *149*, 109−119. (g) Sagstuen, E.; Hole, E. O.; Nelson, W. H.; Close, D. M. *J. Phys. Chem.* **1992**, *96*, 8269−8276. (h) Schaefer, A.; Hüttermann, J.; Kraft, G. *Int. J. Radiat. Biol.* **1993**, *63*, 139−149.

(4) (a) Bernhard, W. A.; Farley, R. A. *Radiat. Res.* **1976**, *66*, 189−198. (b) Spaletta, R. A.; Bernhard, W. A. *Radiat. Res.* **1982**, *89*, 11−24. (c) Barnes, J.; Bernhard, W. A. *J. Phys. Chem.* **1993**, *97*, 3401−3408. (d) Barnes, J. P.; Bernhard, W. A. *J. Phys. Chem.* **1994**, *98*, 887−893. (e) Bernhard, W. A.; Mroczka, N.; Barnes, J. *Int. J. Radiat. Biol.* **1994**, *66*, 491−497. (f) Naumov, S.; Hildebrand, K.; Von Sonntag, C. *J. Chem. Soc., Perkin Trans. 2* **2001**, 1648−1653. (g) Debije, M. G.; Bernhard, W. A. *J. Phys. Chem. A* **2002**, *106*, 4608−4615.

(5) Wetmore, S. D.; Himo, F.; Boyd, R. J.; Eriksson, L. A. *J. Phys. Chem. B* **1998**, *102*, 7484−7491.

(6) Close, D. M.; Eriksson, L. A.; Hole, E. O.; Sagstuen, E.; Nelson, W. H. *J. Phys. Chem. B* **2000**, *104*, 9343−9350.

(7) Podmore, I. D.; Malone, M. E.; Symons, M. C. R.; Cullis, P. M.; Dalgarno, B. J. *J. Chem. Soc., Faraday Trans.* **1991**, *87*, 3647−3652.

(8) (a) Steenken, S.; Jagannadham, V. *J. Am. Chem. Soc.* **1985**, *107*, 6818−6826. (b) Hazra, D. K.; Steenken, S. *J. Am. Chem. Soc.* **1983**, *105*, 4380−4386.

(9) (a) Tureček, F. *J. Mass. Spectrom.* **1998**, *33*, 779−795. (b) Wolken, J. K.; Syrstad, E. A.; Vivekananda, S.; Tureček, F. *J. Am. Chem. Soc.* **2001**, *123*, 5804−5805.

(10) (a) Syrstad, E. A.; Vivekananda, S.; Tureček, F. *J. Phys. Chem. A* **2001**, *105*, 8339−8351. (b) Wolken, J. K.; Tureček, F. *J. Phys. Chem. A* **2001**, *105*, 8352−8360. (c) Tureček, F.; Wolken, J. K. *J. Phys. Chem. A* **2001**, *105*, 8740−8747.

(11) (a) Nguyen, V. Q.; Tureček, F. *J. Mass Spectrom.* **1996**, *31*, 1173−1184. (b) Nguyen, V. Q.; Tureček, F. *J. Mass Spectrom.* **1997**, *32*, 55−63. (c) Nguyen, V. Q.; Tureček, F. *J. Am. Chem. Soc.* **1997**, *119*, 2280−2290. (d) Frøsig, L.; Tureček, F. *J. Am. Soc. Mass. Spectrom.* **1998**, *9*, 242−254. (e) Tureček, F.; Wolken, J. K.; Sadílek, M. *Eur. Mass Spectrom.* **1998**, *4*, 321−332. (f) Tureček, F.; Wolken, J. K. *J. Phys. Chem. A* **1999**, *103*, 1905−1912. (g) Wolken, J. K.; Tureček, F. *J. Am. Chem. Soc.* **1999**, *121*, 6010−6018. (h) Wolken, J. K.; Tureček, F. *J. Phys. Chem. A* **1999**, *103*, 6268−6281.

(12) Tureček, F. *Top. Curr. Chem.* **2003**, *225*, 75−127.

(13) (a) Szczesniak, M.; Szczepaniak, K.; Kwiatkowski, J. S.; Kubulat, K.; Person, W. B. *J. Am. Chem. Soc.* **1988**, *110*, 8319−8330. (b) Kobayashi, R. *J. Phys. Chem. A* **1998**, *102*, 10813−10817. (c) Fogarasi, G. *J. Mol. Struct.* **1997**, *413*−*414*, 271−278. (d) Hall, R. J.; Burton, N. A.; Hiller, I. H.; Young, P. E. *Chem. Phys. Lett.* **1994**, *220*, 129−132.

(14) Polce, M. J.; Wesdemiotis, C.; Tureček, F.; Wolken, J. K. unpublished data.

(15) (a) Rossi, M.; Kistenmacher, T. J. *Acta Crystallogr.* **1977**, *B33*, 3962−3965. (b) Nowak, M. J.; Lapinski, L.; Fulara, J. *Spectrochim. Acta, Part A: Mol. Biomol. Spectrosc.* **1989**, *45A*, 229−242. (c) Brown, R. D.; Godfrey, P. D.; McNaughton, D.; Pierlot, A. P. *J. Am. Chem. Soc.* **1989**, *111*, 2308−2310.

(16) (a) Trygubenko, S. A.; Bogdan, T. V.; Rueda, M.; Orozco, M.; Luque, F. J.; Šponer, J.; Slavíček, P.; Hobza, P. *Phys. Chem. Chem. Phys.* **2002**, *4*, 4192−4203. (b) Fogarasi, G.; Szalay, P. G. *Chem. Phys. Lett.* **2002**, *356*, 383−390. (c) Sambrano, J. R.; de Souza, A. R.; Queralt, J. J.; Andres, J. *Chem. Phys. Lett.* **2000**, *317*, 437−443. (d) Morpurgo, S.; Bossa, M.; Morpurgo, G. O. *Adv. Quantum Chem.* **1999**, *36*, 169−183. (e) Gorb, L.; Leszczynski, J. *Int. J. Quantum Chem.* **1998**, *70*, 855−862. (f) Paglieri, L.; Corongiu, G.; Estrin, D. A. *Int. J. Quantum Chem.* **1995**, *56*, 615−625. (g) Destexhe, A.; Smets, J.; Adamowicz, L.; Maes, G. *J. Phys. Chem.* **1994**, *98*, 1506−1514. (h) Gould, I. R.; Darren, V. S.; Young, P.; Hillier, I. H. *J. Org. Chem.* **1992**, *57*, 4434−4437. (i) McClure, R. J.; Craven, B. M. *Acta Crystallogr.* **1973**, *B29*, 1234−1238. (j) Weber, H. P.; Craven, B. M.; McMullan, R. K. *Acta Crystallogr.* **1980**, *B36*, 645−649.

(17) Colson, A.-O.; Becker, D.; Eliezer, I.; Sevilla, M. D. *J. Phys. Chem. A* **1997**, *101*, 8935−8941.

(18) Adamo, C.; Heitzmann, M.; Meilleur, F.; Rega, N.; Scalmani, G.; Grand, A.; Cadet, J.; Barone, V. *J. Am. Chem. Soc.* **2001**, *123*, 7113−7117.

(19) Naumov, S.; Barthel, A.; Reinhold, J.; Dietz, F.; Geimer, J.; Beckert, D. *Phys. Chem. Chem. Phys.* **2000**, *2*, 4207−4211.

(20) See for example: (a) Lynch, B. J.; Fast, P. L.; Harris, M.; Truhlar, D. G. *J. Phys. Chem A* **2000**, *104*, 4811−4815. (b) Rice, B. M.; Pai, S. V.; Chabalowski, C. F. *J. Phys. Chem. A* **1998**, *102*, 6950−6956. (c) Skokov, S.; Wheeler, R. A. *Chem. Phys. Lett.* **1997**, *271*, 251−258. (d) Basch, H.; Hoz, S. *J. Phys. Chem. A* **1997**, *101*, 4416−4431. (e) Nguyen, M. T.; Creve, S.; Vanquickenborne, L. G. *J. Phys. Chem.* **1996**, *100*, 18422−18425. (f) Jursic, B. *Chem. Phys. Lett.* **1996**, *256*, 603−608. (g) Wong, M. W.; Radom, L. *J. Phys. Chem.* **1995**, *99*, 8582−8588.

(21) Tureček, F. *J. Phys. Chem. A* **1998**, *102*, 4703−4713.

(22) (a) Carpenter, F. H.; Tureček, F. *J. Chem. Soc., Perkin Trans. 2* **1999**, 2315−2323. (b) Tureček, F.; Polášek, M.; Frank, A. J.; Sadílek, M. *J. Am. Chem. Soc.* **2000**, *122*, 2361−2370. (c) Polášek, M.; Tureček, F. *J. Am. Chem. Soc.* **2000**, *122*, 9511−9524. (d) Vivekananda, S.; Wolken, J. K.; Tureček, F. *J. Phys. Chem. A* **2001**, *105*, 9130−9141. (e) Srikanth, R.; Bhanuprakash, K.; Srinivas, R.; Vivekananda, S.; Syrstad, E. A.; Tureček, F. *J. Am. Soc. Mass Spectrom.* **2002**, *13*, 250−264. (f) Vivekananda, S.; Tureček, F.; Polášek, M. *J. Mass Spectrom.* **2002**, *37*, 829−839. (g) Tureček, F.; Syrstad, E. A. *J. Am. Chem. Soc.* **2003**, *125*, 3353−3369.

(23) Rassolov, V. A.; Ratner, M. A.; Pople, J. A. *J. Chem. Phys.* **2000**, *112*, 4014−4019.

(24) Frisch, M. J.; Trucks, G. W.; Schlegel, H. B.; Scuseria, G. E.; Robb, M. A.; Cheeseman, J. R.; Zakrzewski, V. G.; Montgomery, J. A., Jr.; Stratmann, R. E.; Burant, J. C.; Dapprich, S.; Millam, J. M.; Daniels, A. D.; Kudin, K. N.; Strain, M. C.; Farkas, O.; Tomasi, J.; Barone, V.; Cossi, M.; Cammi, R.; Mennucci, B.; Pomelli, C.; Adamo, C.; Clifford, S.; Ochterski, J.; Petersson, G. A.; Ayala, P. Y.; Cui, Q.; Morokuma, K.; Malick, D. K.; Rabuck, A. D.; Raghavachari, K.; Foresman, J. B.; Cioslowski, J.; Ortiz, J. V.; Stefanov, B. B.; Liu, G.; Liashenko, A.; Piskorz, P.; Komaromi, I.; Gomperts, R.; Martin, R. L.; Fox, D. J.; Keith, T.; Al-Laham, M. A.; Peng, C. Y.; Nanayakkara, A.; Gonzalez, C.; Challacombe, M.; Gill, P. M. W.; Johnson, B. G.; Chen, W.; Wong, M. W.; Andres, J. L.; Head-Gordon, M.; Replogle, E. S.; Pople, J. A. *Gaussian 98*; Gaussian, Inc.: Pittsburgh, PA, 1998.

(25) (a) Becke, A. D. *J. Chem. Phys.* **1993**, *98*, 1372, 5648. (b) Stephens, P. J.; Devlin, J. J.; Chabalowski, C. F.; Frisch, M. J. *J. Phys. Chem.* **1994**, *98*, 11623.

(26) Møller, C.; Plesset, M. S. *Phys. Rev.* **1934**, *46*, 618−622.

(27) Schlegel, H. B. *J. Chem. Phys.* **1986**, *84*, 4530−4534.

(28) Cížek, J.; Paldus, J.; Šroubková, L. *Int. J. Quantum Chem.* **1969**, *3*, 149−167.

(29) Laidler, K. J.; King, M. C. *J. Phys. Chem.* **1983**, *87*, 2657.

(30) Barone, V.; Cossi, M.; Tomasi, J. *J. Chem. Phys.* **1997**, *107*, 3210−3221.

(31) Mulliken, R. S. *J. Chem. Phys.* **1955**, *23*, 1833−1840.

(32) Gai, H.; Garrett, B. C. *J. Phys. Chem.* **1994**, *98*, 9642−9648.